Identification of Parameters in Polymer Crystallization, Semiconductor Models and Elasticity via Iterative Regularization Methods

Heinz W.Engl*

Industrial Mathematics Institute
Johannes–Kepler–Universität
Linz, Austria

1 Introduction

The identification of parameters in (partial) differential equations from measurements of the solution is an important step in many modelling problems. Mathematically, it is a (usually ill–posed) inverse problem which needs some regularization in order to cope with noise in the data. We present industrially relevant parameter identification problems from the areas of polymer growth, semiconductor modelling and elasticity and put these problems into the functional–analytic framework of ill–posed nonlinear operator equations in Hilbert spaces. In this framework, we discuss regularization methods with a special emphasis on iterative regularization methods. One of these methods, namely Landweber iteration, is used to solve the three parameter identification problems numerically. The first two problems are mildly and severely ill–posed, respectively, while the third problem has the new feature of containing also second derivatives of the unknown parameter which leads to some questions which are not yet completely understood.
It gives us special pleasure to present this paper in a volume dedicated to Prof.Lavrentiev due to the many contributions that Russian mathematicians, among them quite prominently Prof.Lavrentiev and his school, have made to the field of inverse problems.

*Acknowledgements: This work was supported by the Austrian Science Foundation FWF (projects P13478-INF and F1308). The work reported in Section 7 was performed while the author was at the Oxford Centre for Industrial and Applied Mathematics and supported by the EPSRC grant GB/B06793/01. Discussions with David Allwright, David Gelder, John Ockendon and Domingo Salazar are gratefully acknowledged.

2 An Example: Identification of the Nucleation Rate in Polymer Crystallization

In [8], the following (one-dimensional) mathematical model for the non-isothermal crystallization of polymers was developed (see also [9] and [10] for higher dimension):

$$\frac{\partial T}{\partial t} = D\frac{\partial^2 T}{\partial x^2} + L\frac{\partial \xi}{\partial t} \tag{1}$$

$$\frac{\partial}{\partial t}\left(\frac{1}{\widetilde{G}(T)(1-\xi)}\frac{\partial \xi}{\partial t}\right) = \frac{\partial}{\partial x}\left(\frac{\widetilde{G}(T)}{1-\xi}\frac{\partial \xi}{\partial x}\right) + 2\frac{\partial}{\partial t}(\widetilde{N}(T)) \tag{2}$$

with initial conditions

$$T(x,0) = T^0(x) \tag{3}$$

$$\xi(x,0) = 0 \tag{4}$$

$$\frac{\partial \xi}{\partial t}(x,0) = 0 \tag{5}$$

and boundary conditions

$$\frac{\partial T}{\partial n}(x,t) = \alpha(T(x,t) - T^1(x,t))\ for\ x \in \partial\Omega \tag{6}$$

$$\frac{\partial \xi}{\partial t}(x,t) + \widetilde{G}(T)\frac{\partial \xi}{\partial n}(x,t) = 0\ for\ x \in \partial\Omega, \tag{7}$$

where T denotes the temperature, ξ the degree of crystallinity, $\tilde{G}$ the radial growth rate of a nucleus and $\tilde{N}$ the nucleation rate per unit length (dependent on temperature).

The diffusion coefficient D, the latent heat L and the heat transfer coefficient α can be determined experimentally, as can sometimes the radial growth rate $\tilde{G}$. The aim is to identify the temperature-dependent nucleation rate $\tilde{N}$. This can be seen as the identification of the nonlinearity $\tilde{N} = \tilde{N}(T)$ in the coupled parabolic–hyperbolic system (1), (2). An important question in such an identification problem, which has to be posed to the practitioners before doing mathematics, is which data are available. Here, the experimentally available data are:

- the temperature development at the boundary

$$T(x,t), x \in \partial\Omega, t \in [0,t^*] \tag{8}$$

  and

- the final degree of crystallinity

$$\xi(x,t^*), x \in \Omega. \tag{9}$$

We are dealing with a nonlinear inverse problem, which we first put into the abstract formulation of an operator equation:

Let F denote the operator mapping a **given** nucleation rate to the data described above. F cannot be computed explicitly, but evaluating F involves

- solving the (nonlinear) parabolic–hyperbolic system (1)-(7) for T, ξ
- applying trace operators to obtain the calculated data (8), (9) for a given $\tilde{N}$.

Now, the inverse problem of determining $\tilde{N}$ amounts to solving the nonlinear operator equation

$$F(\tilde{N}) = (\text{noisy) data}.$$

The problem of identifying the nucleation rate was treated in this framework in [11], we come back to it later after having given an overview over the abstract theory of nonlinear ill–posed operator equations, which is needed for an appropriate treatment of our identification problem.

3 Functional–Analytic Theory of Nonlinear Ill–Posed Problems

As a model for nonlinear ill-posed problems, we consider an operator equation

$$F(x) = y_0,$$

where $F : D(F) \subset X \to Y$ is a nonlinear operator between Hilbert spaces X and Y. The basic assumptions on F needed for a reasonable theory, which we will always make, are that F is continuous and that F is weakly (sequentially) closed, i.e., for any sequence $\{x_n\} \subset D(F)$, weak convergence of x_n to x in X and weak convergence of $F(x_n)$ to y in Y imply that $x \in D(F)$ and $F(x) = y$.

Here, F is the "forward operator" for an inverse problem, i.e., the operator describing the corresponding direct problem. In Section 2, F was the operator mapping a given nucleation rate to the data (8), (9). More general, F is the operator mapping a given parameter in a PDE to the solution of the PDE with this parameter if our inverse problem is a parameter identification problem. In an inverse scattering problem, where we want to determine an obstacle from measuring a wave scattered by this obstacle, F maps the domain describing the obstacle to the far field in a scattering problem as determined by the Helmholtz or Maxwell equations in the exterior of that domain with an appropriate radiation condition (cf. [15],[31]).
By definition, an inverse problem need not have a solution, and the solution need not be unique. In the linear case, one reacts to these difficulties by defining a "best–approximate

solution" as a least–squares solution of minimal norm (cf. [26], [32]). In the nonlinear setting, the corresponding notion of a "solution" is the concept of an "x^*–minimum–norm–least–squares solution x_0" introduced in [18] defined by the two consecutive minimization problems

$$\|F(x_1) - y_0\| = \min\{\|F(x) - y_0\| / x \in D(F)\}$$

and

$$\|x_0 - x^*\| = \min\{\|x - x^*\| / \|F(x) - y_0\| = \|F(x_1) - y_0\|\}.$$

Such an x_0 need not exist and, as opposed to the linear case, even if it exists, it need not be unique. The choice of x^* is crucial: It plays the role of a selection criterion determining which among possibly many solutions is sought for, available a–priori information about the unknown solution (e.g., about discontinuities in the solution or, in its derivatives) should be entered into x_0 (which is easier said than done).

The following and many more results with proofs can be found in [32].

In the linear case, a problem is ill–posed if the forward operator is compact and has infinite–dimensional range, for which it is sufficient that the operator is compact, injective and defined on an infinite–dimensional Hilbert space. The following result shows that compactness and local injectivity imply ill-posedness also in the nonlinear case:

Proposition 3.1. *Let F be compact, $F(x_0) = y_0, x_0 \in \operatorname{int} D(F)$, $F(x) = y$ be uniquely solvable in a neighborhood of y_0, and $\dim X = \infty$. Then F^{-1} is discontinuous in y_0.*

If we have noisy data, then we have to regularize (stabilize) the problem, since just applying F^{-1} to noisy data would not give a useful result due to the discontinuity. To be specific, we assume that instead of y_0, we have noisy data y^δ and assume that δ is a norm bound for the error, i.e.,

$$\|y_0 - y^\delta\| \leq \delta$$

holds.
In the linear setting, the (related) regularization methods of Lavrentiev (see [35], [40]) and of Tikhonov ([43], [26]) are among the most widely–used and successful ones. Tikhonov regularization can formally be carried over to the nonlinear setting via its variational formulation by combining the two minimization steps involved in the definition of an "x^*–minimum–norm–least–squares solution x_0" into one minimization step, where the functional to be minimized is a weighted sum of the squares of the two original functionals, the weight being called the "regularization parameter":

$$\|F(x) - y^\delta\|^2 + \alpha\|x - x^*\|^2 \to \text{min. over } D(F).$$

We denote any minimizer by x_α^δ . Under our general assumptions about F, such a minimizer exists, but in contrast to the linear case, it need not be unique. In the linear case, spectral theory in Hilbert space is a powerful tool for analyzing convergence of various regularization

methods (cf. e.g. [32]); in the nonlinear setting, this tool is not available, so that proofs of results about convergence, stability and convergence rates of regularization methods for nonlinear ill–posed problems are much more complicated. It was shown in [42] that for $\alpha > 0$, Tikhonov regularization is stable (in a multi–valued sense, since minimizers need not be unique) and that, if the regularization parameter is chosen such that $\alpha = \alpha(\delta) \to 0$ and $\frac{\delta^2}{\alpha} \to 0$, then x_α^δ converges (again in a multi–valued sense) to an x^*–minimum–norm–solution x_0 of $F(x) = y_0$, if this equation has a solution; for the case that is has only a least–squares solution see [5].
The following result about convergence rates has been proven in [18]:

Theorem 3.2. *Let $D(F)$ be convex and let x_0 be an x^*–minimum–norm–solution. Assume furthermore that*

(i) F is Fréchet–differentiable,

(ii) there exists an $L > 0$ with $\|F'(x_0) - F'(z)\| \leq L\|x_0 - z\|$ for all $z \in D(F)$,

(iii) there exists a $w \in Y$ with $x_0 - x^* = F'(x_0)^* w$,

(iv) $L\|w\| < 1$.

Then, for $\alpha \sim \delta$,

$$\|x_\alpha^\delta - x_0\| = O(\sqrt{\delta}).$$

The parameter choice rule in that Theorem is a so-called "a–priori rule", since it is chosen just as a function of the noise level; a parameter choice rule that depends on the noise level and on the actual data y^δ is called an "a–posteriori rule". For a–posteriori parameter choice rules for Tikhonov regularization which always lead to optimal convergence rates see [19] for linear and [20] for nonlinear ill–posed problems.
It is well–known (see e.g. [41]) that the convergence of regularization methods is arbitrarily slow if the problem is really ill–posed. Convergence rates can only be obtained under additional conditions on the (unknown) solution of the inverse problem, which are usually given in the form of "source conditions" like

$$x_0 - x^* \in R(F'(x_0)^*) \tag{10}$$

as in Theorem 3.2 (for more general forms and a more thorough discussion, see [32]). For concrete forward operators F, such source conditions usually imply a–priori smoothness assumptions (related to smoothing properties of the forward map F), which explains the numerical experience that only smooth parts of $x_0 - x^*$ can be resolved fast, and boundary conditions, i.e., some boundary information about x_0 (which has then to be incorporated into x^*) has to be known in order to obtain a reasonable convergence rate. Also this can be observed in practice.
The severeness of a source condition depends on the smoothing properties of the forward operator. E.g., for the identification of the diffusion coefficient in a heat equation, (10) essentially means that $x_0 - x^* \in H^2$, the problem is "mildly ill–posed" (cf. [18]), while

for inverse scattering (if x_0 denotes a parameterization of the unknown boundary of the obstacle), not even the analyticity of $x_0 - x^*$ suffices for (10), the problem is "severely ill–posed" (cf. [30]).
In concrete cases, source conditions like (10) are difficult to interpret (see. e.g. [2]): they are conditions about the solvability of an adjoint linearized equation. The main obstacle in the interpretation of source conditions seems to be the adjoint. In [25], a variant of the source condition (10) has been introduced for the problem of identifying $q = q(x)$ in

$$\frac{\partial u}{\partial t} = \text{ div } (q(x) \text{ grad } u).$$

The key idea there is that the adjoint involves the weak form of the PDE describing the forward problem, which gives rise to a more natural source condition which is easier to interpret. This idea has been carried over to the problem of identifying a temperature–dependent diffusion coefficient $q = q(u)$ in

$$-\text{div}(q(u)\text{grad } u) = f(x) \text{ in } \Omega \subseteq \mathbf{R}^n$$

$$u(x) = 0 \qquad \text{on} \quad \partial\Omega$$

from (distributed or boundary) temperature measurements by Tikhonov regularization in [21]. Like in the problem described in Section 2, this can be seen as the "identification of a nonlinearity".
The inverse problems for $q = q(x)$ and $q = q(u)$ are markedly different: On the one hand, in more than one space dimension, the "$q(u)$–problem" seems to be easier due to the fact that q depends only on a one–dimensional variable (as opposed to the multi–dimensional space variable). On the other hand, already the direct problem is nonlinear. But the main numerical problem is that q can be identified at best on the interval which is covered by $u = u(q)$, which is a–priori unknown.
In [21], a convergence rate of $O(\sqrt{\delta})$ for Tikhonov regularization of the "$q(u)$–problem" is shown under a source condition whose interpretation via the "Coarea Formula" ([24]) is, in addition to $q_0 - q^* \in H^4$, that $u(q_0)$ has no isotherms of vanishing $(n-1)$–dimensional Hausdorff measure, which is a reasonable condition since it says that each temperature for which q has to be determined has to be assumed "sufficiently often".
The following numerical results from [21] clearly show that $q(u)$ can be determined only in the temperature interval which is actually assumed, and that it can be determined quite well there even with a rather bad q^*:

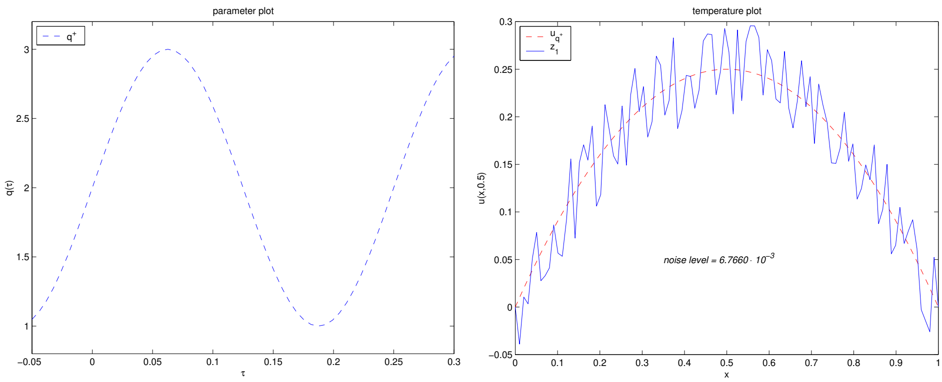

Figure 1: the true parameter q_0 and the noisy data z_1 at t = 0.5

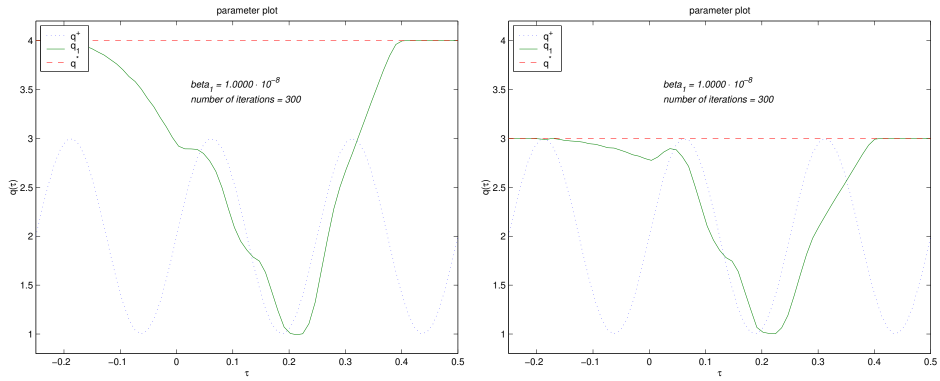

Figure 2: q_1 identified from z_1 with $q^* = 4$ and $q^* = 3$

While for linear problems, Tikhonov and Lavrentiev regularization are certainly methods of choice, Tikhonov regularization has a severe drawback for nonlinear problems: the functional to be minimized is in general not convex, which makes finding a global minimum difficult due to the possible presence of local minima. This makes iterative regularization methods an attractive alternative, although of course also there, one has the problem of local convergence.

4 Iterative Regularization of Nonlinear Ill–Posed Problems

For nonlinear well–posed equations, Newton's method is the basic iterative solution method. It has fast local convergence, can be globalized, the theory is well–developed. But what about Newton's method for ill–posed problems?
The basis of Newton's method is the linearization of $F(x) = y$ at the current iterate x_k:

the next iterate x_{k+1} is determined as solution of

$$F'(x_k)(x - x_k) = -\Big(F(x_k) - y\Big). \tag{11}$$

But for a nonlinear ill–posed problem, the linearization (11) is generally ill–posed: e.g., if F is compact, so is $F'(x_k)$ (see [18] for a discussion about the relations between the ill–posedness of a nonlinear problem and of its linearization). The obvious way to proceed is to solve (11) stably by a regularization method for *linear* equations. If one chooses (linear) Tikhonov regularization for that purpose, one obtains the *Levenberg–Marquardt method*:

$$x_{k+1} = x_k - (F'(x_k)^* F'(x_k) + \alpha_k I)^{-1} F'(x_k)^* (F(x_k) - y^\delta)$$

with $\alpha_k \to 0$ as $k \to \infty$, $\|y - y^\delta\| \le \delta$.
For well–posed problems, a complete analysis of the Levenberg–Marquardt method has long been available; convergence for ill–posed problems has been proven in [27]. A variant is the *iteratively regularized Gauß–Newton method:*

$$x_{k+1} = x_k - (F'(x_k)^* F'(x_k) + \alpha_k I)^{-1} [\Big(F'(x_k)^* (F(x_k) - y^\delta) + \alpha_k (x_k - \zeta)\Big)].$$

The additional last term provides additional stabilization by anchoring the iterates to ζ (however, weaker as the iteration progresses). Convergence with rates have been shown in [3] and [28].
One can also use an iterative method for solving the linear problem (11), which leads to nested iterations (see [33],[34], [39]).
In any iterative method for solving a (linear or nonlinear) ill–posed problem, it is crucial to stop the iteration at at the right step, the "stopping index" $n = n(\delta, y^\delta)$ plays the role of the regularization parameter in Tikhonov regularization. For proving convergence rates, one needs again source conditions like (10) and conditions restricting the nonlinearity of F (see [29] and [16] for a discussion of such conditions).
For well–posed nonlinear equations, invariance properties have been used for the systematic development of a convergence theory for Newton–like methods (see [17]). In [16], such an approach could also be developed for ill–posed problems:
The unregularized Newton method (in the form of the normal equation)

$$x_{k+1} = x_k - \Big(F'(x_k)^* F'(x_k)\Big)^{-1} \Big(F'(x_k)^* \Big(F(x_k) - y\Big)\Big) \tag{12}$$

is invariant under affine transformations of $G(x) := F'(x)^* \Big(F(x) - y\Big)$ and under unitary transformations of F. As noted above, for ill–posed problems, (12) is usually unstable, so that $(F'(x)^* F'(x))^{-1}$ has to be replaced by a continuous operator. There are several possibilities:

(1) If $(F'(x)^*F'(x))^{-1}$ is replaced (in an extremely crude way) simply by I, one obtains a method which we will discuss below in several applications, called the *(damped) Landweber method*

$$x_{k+1} = x_k - \omega F'(x_k)^* \Big(F(x_k) - y^\delta \Big).$$

(2) If $(F'(x_k)^*F'(x_k))^{-1}$ is replaced by $(\alpha_k I + F'(x_k)^*F'(x_k))^{-1}$, one obtains the *Levenberg–Marquardt method.*

(3) The Levenberg–Marquardt method augmented by the term

$$-(\alpha_k I + F'(x_k)^*F'(x_k))^{-1}\alpha_k(x_k - \zeta)$$

for additional stabilization leads to the *iteratively regularized Gauß–Newton method.*

The basic condition used for the convergence analysis is the "Newton–Mysovskii–condition"

$$\|(F'(x) - F'(x^\dagger))F'(x^\dagger)^\#\| \le C_{NM}\|x - x^\dagger\|$$

with a left inverse $F'(x^\dagger)^\#$; in order to avoid confusion with the starting value x_0 of the iteration, we use $x^\dagger$ as symbol for the true solution.
Under a Newton–Mysovskii–condition, one can prove the following result for the iteration x_k^δ defined via the damped Landweber method:

Theorem 4.1. *If*

$$x^\dagger - x_0 = (F'(x^\dagger)^*F'(x^\dagger))^\nu w$$

for some $0 < \nu \le \frac{1}{2}$ *and* $\|w\|$ *is sufficiently small, then*

$$\|x^\dagger - x_k^\delta\| \le c_*\|w\|(k+1)^{-\nu}$$

for $0 \le k < k_*$*, where the stopping index* k_* *is defined via the "discrepancy principle"*

$$\|y^\delta - F(x_{k_*})\| \le \tau\delta < \|y^\delta - F(x_k^\delta)\|\,, \quad 0 \le k \le k_*\,,$$

with a suitable $\tau > 2$.
For $\delta = 0$*, this rate holds for all* k*. Otherwise,*

$$\|x_{k_*}^\delta - x^\dagger\| = O\left(\delta^{\frac{2\nu}{1+2\nu}}\right).$$

For $\nu = \frac{1}{2}$, we obtain a source condition $x^\dagger - x_0 \in R(F'(x^\dagger)^*)$ similar to (10) and a convergence rate $O(\sqrt{\delta}))$.
A systematic treatment of many iterative methods for solving nonlinear ill–posed problems can be found in [23].

5 Identification of the Nucleation Rate in Polymer Crystallization by Landweber Iteration

We return to the problem of identifying the nucleation rae $\tilde{N}$ in

$$\begin{aligned}\frac{\partial T}{\partial t} &= D\frac{\partial^2 T}{\partial x^2} + L\frac{\partial \xi}{\partial t}\\ \frac{\partial}{\partial t}\left(\frac{1}{\widetilde{G}(T)(1-\xi)}\frac{\partial \xi}{\partial t}\right) &= \frac{\partial}{\partial x}\left(\frac{\widetilde{G}(T)}{1-\xi}\frac{\partial \xi}{\partial x}\right) + 2\frac{\partial}{\partial t}(\widetilde{N}(T))\end{aligned}$$

defined in Section 2 and recall the availabe data:

- the temperature development at the boundary

$$T(x,t), x \in \partial\Omega, t \in [0,t^*]$$

- the final degree of crystallinity

$$\xi(x,t^*), \quad x \in \Omega.$$

By defining F as the operator taking $\tilde{N}$ to the data, the problem can be viewed in the abstract framework of Sections 3 and 4, and Landweber iteration can be formally applied. The operator $F'(\tilde{N}_k)^*$ appearing in the iteration can be characterized by linear system of PDE's (see [11] for details). The source condition $\tilde{N}^\dagger - \tilde{N}_0 \in R(F'(\tilde{N}_0)^*)$ can be interpreted as requiring that $\tilde{N}^\dagger - \tilde{N}_0 \in H^2$, which means that if we want a reasonable convergence rate, we have to incorporate details of $\tilde{N}^\dagger$ which are less smooth than H^2 into the initial guess $\tilde{N}_0$; in addition, the source condition includes boundary conditions for $\tilde{N}^\dagger - \tilde{N}_0$ that can be fulfilled if the experiment covers the whole temperature range from the melting point down to the glass transition temperature.
Our numerical tests confirm these predictions from the theory: The convergence rate $O(\sqrt{\delta})$ can be numerically verified for data covering the whole temperature range, while for a restricted temperature range, convergence is slower. Also, the role of the stopping rule (which was done according to the discrepancy principle described in Theorem 4.1) can be seen quite dramatically; the following figures show results with 1 % error in the data:

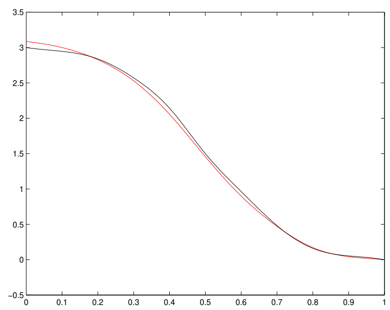

Figure 3: Exact solution vs. determined solution at iterate k_*

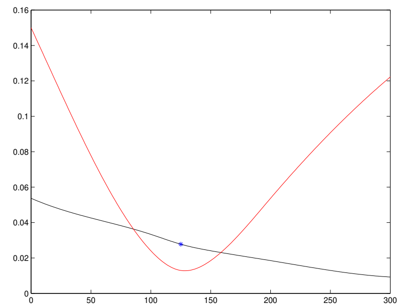

Figure 4: Residual (lower curve), error (upper curve) as function of iteration index. $*$: stopping index

While the residual decreases steadily as the iteration progresses, the error between the iterates and the exact solution first decreases, but then increases quite fast again; this turn appears close to the stopping index determined by the discrepancy principle.
In [7], the iteratively regularized Gauß–Newton method (IRGN) has been used for the same problem. While it was faster for exact data, the instability (i.e., the rise in the error just described) appeared earlier, which compensates the faster convergence. Thus, in the presence of noise, a theoretically faster method like IRGN need not be advantageous over the Landweber method, which is much simpler to implement (and cheaper since the iteration involves no inversion of an operator, in contrast to IRGN). Based on this observation, we used Landweber iteration also for other inverse problems with good results. While the problem described in this Section was mildly ill–posed, we now report about our experience with Landweber iteration for a severely ill–posed problem.

6 Identification of Doping Profiles in Semiconductor Equations

The results surveyed in this Section are joint work with Martin Burger, Peter Markowich and Paola Pietra and are published in [12]. They concern the identification of the doping profile in the stationary semiconductor equations (based on the drift–diffusion model) and show close relations to impedance tomography; we believe that [12] gives directions for many possible inverse problems to be studied in the future.
To set the stage, we first have to present the stationary drift–diffusion equations; for details, we refer to [37].
Let V denote the electrostatic potential, n the electron density, p the hole density, q the elementary charge. By μ_n and μ_p, we denote the electron and hole mobilities, by D_n and D_p the electron and hole diffusion coefficients, respectively, and by ϵ_s the semiconductor permittivity. We assume that the recombination–generation rate R has the form

$R = F(n,p,x) \cdot (np - n_i^2)$ with $F \geq 0, n_i$ being the intrinsic carrier density. The quantity which we finally want to determine is the *doping profile* C, i.e., the density difference between ionized donors and acceptors.
With this notation, the stationary drift–diffusion equations read as follows:

$$\begin{aligned}
\operatorname{div}(\epsilon_s \nabla V) &= q(n - p - C) && \text{in } \Omega && \text{(Poisson equation)}\\
\operatorname{div}(D_n \nabla n - \mu_n n \nabla V) &= R && \text{in } \Omega && \text{(electron continuity equation)}\\
\operatorname{div}(D_p \nabla p + \mu_p p \nabla V) &= R && \text{in } \Omega && \text{(hole continuity equation),}
\end{aligned}$$

with the following boundary conditions:

- homogeneous Neumann conditions on $\partial\Omega_N \subseteq \partial\Omega$
- on $\partial\Omega_D$ (assumed to have positive measure in $\partial\Omega$):

$$\begin{aligned}
V(x) &= V_D(x) = U(x) + V_{bi}(x) = U(x) + U_T \ln\left(\frac{n_D(x)}{n_i}\right)\\
n(x) &= n_D(x) = \frac{1}{2}\left(C(x) + \sqrt{C(x)^2 + 4n_i^2}\right)\\
p(x) &= p_D(x) = \frac{1}{2}\left(-C(x) + \sqrt{C(x)^2 + 4n_i^2}\right).
\end{aligned}$$

Here, U_T denotes the thermal voltage and U the applied potential.
The standard assumption that the "Einstein relations"

$$D_n = \mu_n U_T, \qquad D_p = \mu_p U_T, \tag{13}$$

hold enables the transformation of this system into "Slotboom variables" u and v via

$$n = C_0 \delta^2 e^{V/U_T} u, \qquad p = C_0 \delta^2 e^{-V/U_T} v \tag{14}$$

with the scaling parameter

$$\delta^2 = \frac{n_i}{C_0},$$

where C_0 is a typical value for the doping profile.
Transformation into dimensionless form with scaled length $\frac{x}{L}$ (where L is a typical device length), scaled mobilities

$$\tilde{\mu}_n = \frac{U_T}{L}\mu_n \qquad \text{and} \qquad \tilde{\mu}_p = \frac{U_T}{L}\mu_p,$$

and rescaled potential $\frac{V}{U_T}$ yields (for constant ϵ_s):

$$
\begin{aligned}
\lambda^2 \Delta V &= \delta^2(e^V u - e^{-V} v) - C && \text{in } \Omega && (15)\\
\operatorname{div} J_n &= \delta^4 Q(u,v,V,x)(uv-1) && \text{in } \Omega && (16)\\
\operatorname{div} J_p &= -\delta^4 Q(u,v,V,x)(uv-1) && \text{in } \Omega && (17)\\
J_n &= \tilde{\mu}_n \delta^2 e^V \nabla u && \text{in } \Omega && (18)\\
J_p &= -\tilde{\mu}_p \delta^2 e^{-V} \nabla v && \text{in } \Omega && (19)
\end{aligned}
$$

with

$$\lambda^2 = \frac{\epsilon_s U_T}{q C_o L^2},$$

$Q(u,v,V,x) = F(n,p,x)$; J_n, J_p are the scaled electron and hole current densities, respectively.
The transformed boundary conditions are:

- on $\partial\Omega_N : \frac{\partial V}{\partial \nu} = 0,\ J_n \cdot \nu = 0,\ J_p \cdot \nu = 0$
- on $\partial\Omega_D : u = e^{-U}, v = e^{U}$,

$$V = U + V_{bi} = U + \ln\left(\frac{1}{2\delta^2}(C + \sqrt{C^2 + 4\delta^2})\right).$$

In this dimensionless form, λ and δ can be used (by letting them tend to 0) to construct reduced models. For this and existence, uniqueness, and regularity of solutions see e.g. [37]. E.g., if

$$C \in \mathcal{D} := \left\{ \ C \in L^2(\Omega) \mid \underline{C} \le C \le \overline{C} \text{ a.e. in } \Omega \ \right\} \tag{20}$$

holds, then a weak solution

$$(V,u,v,J_n,J_p) \in H^1(\Omega)^3 \times L^2(\Omega)^2 \times L^2(\Omega)^2.$$

exists (under reasonable assumptions on $\partial\Omega$). However, uniqueness holds only for small applied potential U. Thus, we consider the problem "around equilibrium" (i.e., linearized around $U = 0$). The aim is to identify the doping profile C from indirect measurements. The following measurements at a contact Γ_1 are possible:

- the current flow

$$I(\Gamma_1) = \int_{\Gamma_1} (J_n + J_p).d\nu \tag{21}$$

- the mean capacitance

$$\tag{22}$$

which, in both cases, is just one number for each applied potential. Since measurements for small U are strongly correlated, they will in practice not be enough to determine C as a function, but only a smaller number of parameters. Possible remedies are

- to use measurements away from equilibrium; however, there is no sound mathematical theory away from equilibrium yet;
- to consider the transient case (see [7] for first results in this direction).

For a first mathematical analysis and first numerical studies for the *inverse doping problem*, we consider the following idealized data:

Voltage–to–current data are given by measurements of the normal component of the current density $J.\nu = (J_n + J_p).\nu$ on $\Gamma_1 \subset \partial\Omega_D$ for all applied voltages $U \in H^{\frac{3}{2}}(\partial\Omega_D)$ with $\|U\| < r$ for some small $r > 0$.

For capacitance data around equilibrium see [12].

We now consider the problem around equilibrium: For $U = 0$, $u = v = 1$ and $V = V^0$, where V^0 solves the Poisson problem

$$\lambda^2 \Delta V^0 = e^{V^0} - e^{-V^0} - C \qquad \text{in } \Omega \tag{23}$$

$$V^0 = V_{bi} \qquad \text{on } \partial\Omega_D \tag{24}$$

$$\frac{\partial V^0}{\partial \nu} = 0 \qquad \text{on } \partial\Omega_N. \tag{25}$$

We linearize the problem around $U = 0$ into direction h and obtain:

$$\lambda^2 \Delta \hat{V} = e^{V^0} \hat{u} - e^{-V^0} \hat{v} + (e^{V^0} + e^{-V^0}) \hat{V} \qquad \text{in } \Omega \tag{26}$$

$$\operatorname{div}\left(\mu_n e^{V^0} \nabla \hat{u}\right) = Q_0(V^0, x)(\hat{u} + \hat{v}) \qquad \text{in } \Omega \tag{27}$$

$$\operatorname{div}\left(\mu_p e^{-V^0} \nabla \hat{v}\right) = Q_0(V^0, x)(\hat{u} + \hat{v}) \qquad \text{in } \Omega \tag{28}$$

with $Q_0(V^0, x) := Q(1, 1, V^0)$, homogeneous Neumann conditions on $\partial\Omega_N$ and

$$\hat{V} = h \qquad \text{on } \partial\Omega_D \tag{29}$$

$$\hat{u} = -h \qquad \text{on } \partial\Omega_D \tag{30}$$

$$\hat{v} = h \qquad \text{on } \partial\Omega_D. \tag{31}$$

Here, $\hat{u}, \hat{v}$ and hence also $\hat{J}_n$ and $\hat{J}_p$ do not depend on $\hat{V}$. Thus, for these quantities, the linearized Poisson equation is not needed.

We now introduce the notation for the *voltage–to–current map*: For a given doping profile C,

$$\begin{array}{rlcl} \Sigma_C : & B_r(0) \subset H^{\frac{3}{2}}(\partial\Omega_D) & \to & L^2(\Gamma_1) \\ & U & \mapsto & J.\nu|_{\Gamma_1}. \end{array} \tag{32}$$

For sufficiently small U, Σ_C is well–defined and smooth: $\Sigma_C \in C^\infty(B_r(0), L^2(\Gamma_1))$. $\Sigma_C'(U)\Phi$ can be evaluated via solving the linearized drift-diffusion system, e.g.:

$$\mathcal{S}_C\Phi := \Sigma_C'(0)\Phi = \left(\mu_n e^{V_{bi}} \frac{\partial \hat{u}}{\partial \nu} - \mu_p e^{-V_{bi}} \frac{\partial \hat{v}}{\partial \nu}\right)|_{\partial\Omega_D},$$

where $(\hat{u}, \hat{v})$ solves

$$\mathrm{div}\ \left(\mu_n e^{V^0} \nabla \hat{u}\right) = Q_0(V^0, x)(\hat{u} + \hat{v}); \quad \mathrm{div}\ \left(\mu_p e^{-V^0} \nabla \hat{v}\right) = Q_0(V^0, x)(\hat{u} + \hat{v}) \quad \text{in } \Omega \tag{33}$$

$$\hat{u} = -\Phi \qquad \hat{v} = \Phi \qquad \text{on } \partial\Omega_D \tag{34}$$

$$\frac{\partial \hat{u}}{\partial \nu} = 0 \qquad \frac{\partial \hat{v}}{\partial \nu} = 0 \qquad \text{on } \partial\Omega_N, \tag{35}$$

and V^0 solves the (nonlinear) equilibrium Poisson problem.
Note that $\mathcal{S}_C$ is a compact linear operator, i.e., the inverse problem of determining the applied potential from the current (which is not the problem we consider here) would be ill–posed. We want to determine C from Σ_C or from $\mathcal{S}_C$ ("reduced voltage–to–current data").

Since $\mathcal{S}_C$ maps *Dirichlet data* for $(\hat{u}, \hat{v})$ to a *linear combination* of their *Neumann data*, it is similar to the well–known *Dirichlet–to–Neumann map*. Hence, results from it impedance tomography, where one determines e.g. a conductivity from the Dirichlet–to–Neumann map, should have some bearing on the inverse doping problem; below, we give some simple examples for this. E.g., the identification of C from reduced voltage–to–current data can be done in the following two steps:

Identify V^0 in

$$\mathrm{div}\ \left(\mu_n e^{V^0} \nabla \hat{u}\right) = Q_0(V^0, x)(\hat{u} + \hat{v}); \quad \mathrm{div}\ \left(\mu_p e^{-V^0} \nabla \hat{v}\right) = Q_0(V^0, x)(\hat{u} + \hat{v}) \quad \text{in } \Omega$$

$$\hat{u} = -\Phi \qquad \hat{v} = \Phi \qquad \text{on } \partial\Omega_D$$

$$\frac{\partial \hat{u}}{\partial \nu} = 0 \qquad \frac{\partial \hat{v}}{\partial \nu} = 0 \qquad \text{on } \partial\Omega_N.$$

and then compute C from

$$\lambda^2 \Delta V^0 = e^{V^0} - e^{-V^0} - C \qquad \text{in } \Omega.$$

The similarities to impedance tomography are even more strinking in special cases:

The unipolar case: Here, $p = 0$ (i.e., $v \equiv 1$). Determining C from reduced voltage–to–current data on all of $\partial\Omega$ reduces to identifying C in

$$\lambda^2 \Delta V^0 = e^{V^0} - e^{-V^0} - C \qquad \text{in } \Omega \tag{36}$$

$$\text{div } \left(e^{V^0} \nabla \hat{u}\right) = 0 \qquad \text{in } \Omega \tag{37}$$

$$V^0 = V_{bi} \qquad \text{on } \partial\Omega \tag{38}$$

from the Dirichlet–to–Neumann map $\hat{u}|_{\partial\Omega} \to \frac{\partial \hat{u}}{\partial v}|_{\partial\Omega}$; since V^0 is known on $\partial\Omega$, $\frac{\partial \hat{u}}{\partial v}$ can be computed from the current $J = \mu_n e^{V_0} \frac{\partial \hat{u}}{\partial v}$. Thus, identifiability results from impedance tomography can be translated into our situation:

Theorem 6.1. *Let $\Omega \subset \mathbf{R}^2$ be a bounded Lipschitz domain and let $\Gamma_1 = \partial\Omega_D = \partial\Omega$. Then, for two doping profiles C_1 and C_2 in $\mathcal{D}$, the equality $\mathcal{S}_{C_1} = \mathcal{S}_{C_2}$ implies that $C_1 = C_2$.*

This follows from [38] (or from [6] for $C \in L^\infty(\Omega) \cap W^{1,p}(\Omega)$).

Zero–Space Charge Limit: This is the model obtained by letting λ tend to 0. The equilibrium Poisson equation reduces to $\sinh V^0 = 2C$, the linearized equations to

$$\text{div } (\mu_n a \nabla \hat{u}) \;=\; q(a,x)(\hat{u} + \hat{v}) \tag{39}$$

$$\text{div } (\mu_p a^{-1} \nabla \hat{v}) \;=\; q(a,x)(\hat{u} + \hat{v}) \tag{40}$$

with

$$a = a(C) = e^{\text{arsinh}(2C)}, \quad q(a,x) = Q(1, 1, \ln(a), x). \tag{41}$$

The inverse doping problem is then the problem of identifying the parameter a in these equations from $\mathcal{S}_C$.

A practically important special case which we also use for numerical tests is *the $P-N-$Diode*: Here, the domain is split into two subregions

$$\begin{array}{lll} P & \text{where} & C > 0 \\ N & \text{where} & C < 0. \end{array}$$

The curve Γ between P and N is called *$p-n-$junction*.

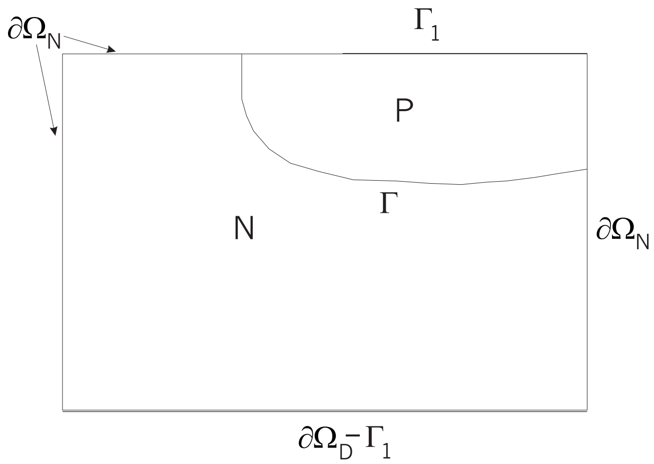

Figure 5: Two-dimensional cross section of a p-n diode.

We assume that C is piecewise constant, there are two Ohmic contacts $\Gamma_1, \Gamma_0 = \partial\Omega_D \backslash \Gamma_1$, and the applied potential has the form

$$U(x) = \begin{cases} U \text{ (constant)} & \text{for } x \in \Gamma_1 \\ 0 & \text{for } x \in \partial\Omega_D - \Gamma_1. \end{cases} \tag{42}$$

The aim is to identify Γ. As data, we use

- the current $I_C(U) := J^U \cdot \nu$ on $\Gamma_1 \subseteq \partial\Omega_D$ for all sufficiently small U

or

- $g_C := \frac{dI_c}{dU}(0)$, which is a function on $\Gamma_1 : g_C(t) = \mathcal{S}_C(t \cdot \chi_{\Gamma_0})$.

In the special limiting case "zero space charge and low injection", i.e., $\lambda \to 0$ and then $\delta \to 0$, a result from [1] implies that Γ is uniquely determined by g_C and that the inverse problem is *severely ill–posed.*

For the numerical solution of determining a $p - n-$junction, we want to use Landweber iteration. For this, the theory presented in Section 4 does not yet suffice, since for severely ill–posed problems, where the forward operator is "exponentially smoothing", i.e., singular values of its linearization decay exponentially, source conditions like

$$x^\dagger - x^* \in R(F'(x^\dagger)^*)$$

are much too strong, Hölder convergence rates like

$$\|x_{k_*}^\delta - x^\dagger\| = O(\sqrt{\delta})$$

cannot be expected. The remedy are "logarithmic" source conditions (to counter exponential smoothing) which yield logarithmic convergence rates:

With the notation of Section 4, we recall the damped Landweber iteration as

$$x_{k+1}^\delta = x_k^\delta - \omega F'(x_k^\delta)^*(F(x_k^\delta) - y^\delta).$$

We then have the following result about logarithmic convergence rates (see [16]):

Theorem 6.2. *Let a Newton–Mysovskii–condition hold. With*

$$f_p(\lambda) := \begin{cases} (1 - \ln\lambda)^{-p} & \textit{for} \quad 0 < \lambda \le 1 \\ 0 & \qquad\quad \textit{else} \end{cases}$$

and $p \ge 1$*, let*

$$x^\dagger - x_0 = f_p(F'(x^\dagger)^* F'(x^\dagger))w$$

hold with $\|w\|$ *sufficiently small. Then*

$$\|x^\dagger - x_k^\delta\| \le c_*(\ln k)^{-p}\,,$$

$$\|y^\delta - F(x_k^\delta)\| \le c_* k^{-1/2}(\ln k)^{-p}$$

and

$$\|x_{k_*}^\delta - x^\dagger\| = O((-\ln\delta)^{-p})$$

hold, if k_* *is defined via the discrepancy principle.*

Analogous results hold also for the iteratively regularized Gauß–Newton method (see [30], [16]. As mentioned in Section 4, a source condition like (10) does not hold in inverse scattering even if the difference between the true obstacle boundary and its a–priori guess is analytic. The use of a logarithmic source condition as in Theorem 6.2 is appropriate here: In [30] (see [31] for more details), the iteratively regularized Gauß–Newton method was used (in H^1) for determining an impenetrable sound–soft obstacle in $\mathbf{R}^2$ from the far–field pattern for one incoming plane wave: Let $x^\dagger$ denote a parameterization of the true boundary, x_0 the initial guess. Then the logarithmic source condition

$$x^\dagger - x_0 \in R(f_p(F'(x^\dagger))^* F'(x^\dagger))$$

(as in Theorem 6.2) means essentially that

$$x^\dagger - x_0 \in H^{1+p},$$

which is perfectly reasonable. The following figures show numerical results. Left, the result after 15 iterations using exact data is shown: the numerical and the true solutions are virtually indistinguishable. The Figure to the right shown the result using data with 5% noise after 3 iterations as obtained from the discrepancy principle: The result is pretty good for a severely ill–posed problem. In both pictures, κ denotes the wave number in the Helmholtz equation, and the unit circle was used as initial guess for the iteration.

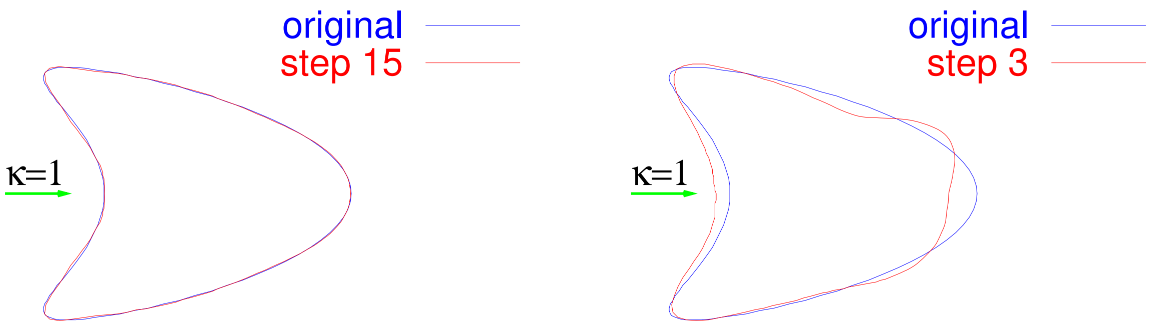

Figure 6:

The convergence rate

$$\|x^{\delta}_{k_*} - x^{\dagger}\|_{H^1} = O((-\ln\delta)^{-p})$$

obtained from the Gauß–Newton analogue of Theorem 6.2 could be verified numerically.

We now return to the numerical solution of the inverse doping problem for a $P{-}N{-}$junction and report on results obtained by Landweber iteration:

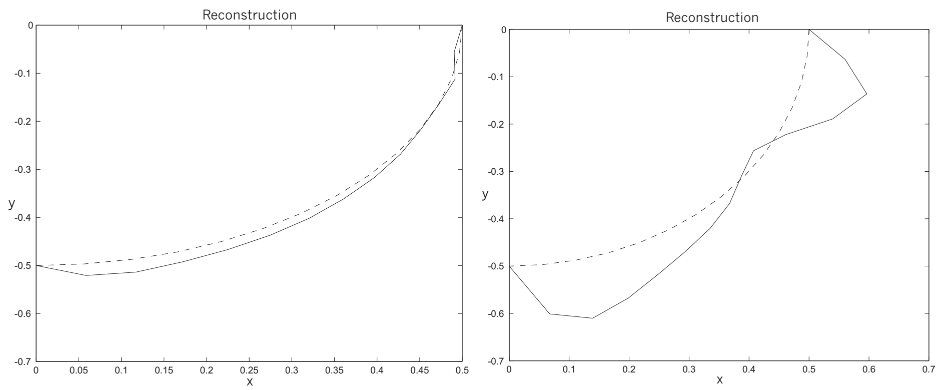

Figure 7: Reconstruction using noisy data from the reduced model for noise levels $\delta = 2.5\%$ (left) and $\delta = 10\%$ (right) compared to the exact junction (dotted).

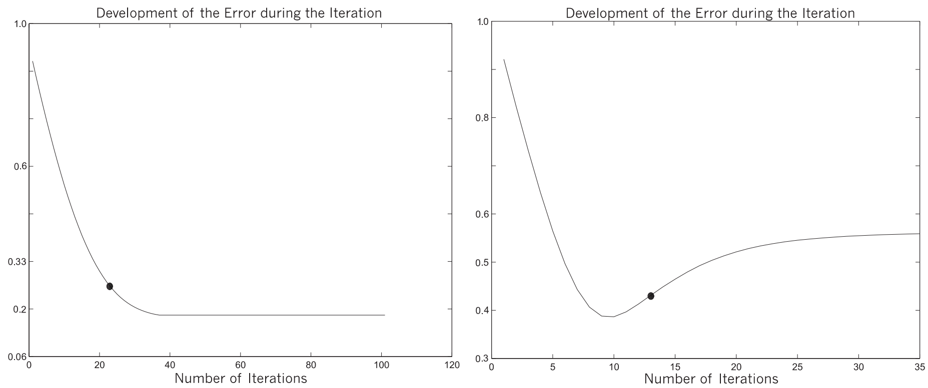

Figure 8: Evolution of the error between reconstruction and exact junction during the iteration, for $\delta = 2.5\%$ (left) and $\delta = 10\%$ (right). The stopping index obtained with the generalized discrepancy principle is marked by a dot.

Similar results were obtained with capacitance data ([12]). For first results using the transient drift–diffusion model, where we have more data due to the time–dimension, see [7].
We close this Section by mentioning that semiconductor models (also more general ones than the drift–diffusion equations) offer a lot of practically important and mathematically interesting inverse problems, where links to the well–developed theory of the Dirichlet–to–Neumann map can be exploited.

7 An Inverse Elasticity Problem from Industry: Windshield Design by Sagging

To manufacture a car wiendshield by the "sagging process", a sheet of glass is put onto a frame and heated, which changes the Young's modulus so that the glass sheet bends due to gravity. The inverse problem is how to heat the glass sheet in order to achieve a desired final shape. Actually, this inverse problem, which can also be viewed as control or optimal design problem, consists of two subproblems:

- to determine the temperature regime from the desired Young's modulus
- to determine the Young's modulus (as a function of position) from the desired displacement.

We consider the second of these inverse problems; for a more detailed description see [22]. The vertical displacement w of the glass (covering, in undeformed state, a two–dimensional domain Ω) satisfies the fourth order equation

$$(E(w_{xx} + \frac{1}{2}w_{yy}))_{xx} + (Ew_{xy})_{xy} + (E(w_{yy} + \frac{1}{2}w_{xx}))_{yy} = -g \ \text{ in } \ \Omega$$

with appropriate boundary conditions on w, where we consider homogeneous Dirichlet conditions here. In reality, lift–off at the frame has to be considered, so that the direct problem leads to a variational inequality (see [36]). The inverse problem is to find the Young's Modulus $E = E(x, y)$ given a desired deformation $\hat{w}$. This can be considered as a PDE for the unknown E:

$$((\hat{w}_{xx} + \frac{1}{2}\hat{w}_{yy})E)_{xx} + (\hat{w}_{xy}E)_{xy} + ((\hat{w}_{yy} + \frac{1}{2}\hat{w}_{xx})E)_{yy} = -g \text{ in } \Omega.$$

Considered as a PDE for E, this equation

- is of second order in E
- changes its type between elliptic and hyperbolic in dependence on $\hat{w}$; in practice, typically both elliptic and hyperbolic regions appear.

The parameter identification problems considered so far were, if considered as PDEs for E, of first order. In this Section, we study the question how the fact that we now have a second order equation influences the numerics (and the analysis) of the parameter identification problem. Furthermore, we ask the same question concerning the type of the PDE in E. We will see that in fact, both phenomena have an influence on the parameter identification problem even if we do not solve it by directly solving the PDE for E (which would amount to the "equation error approach" for solving the parameter identification problem) but by Landweber iteration (which is based on the "output–least–squares approach", cf. [4]). This is somewhat astonishing since in the Landweber iteration formulation, the PDE for E does not even appear. The output–least–squares approach, where we determine E based on the minimization of

$$E \to \|\hat{w} - w_E\|^2,$$

where w_E denotes the solution of the 4th order PDE for given E, is certainly more appropriate since $\hat{w}$ is a target which we want to approximate with some accuracy, while in the equation error approach, there would be no room for a tolerance in $\hat{w}$.
In order to investigate the questions raised above, we consider a "toy problem" which shares with the original problem its key features, but is simpler numerically, since the direct problem is a second order PDE. We have, in the meantime, also started to investigate the full problem, the results are comparable.
We consider the following *direct problem*: Given $E = E(x, y) > 0$, solve the *second* order elliptic PDE

$$-(Ew_x)_x - (Ew_y)_y - (wE_x)_x - E_{yy} = g \text{ in } \Omega$$

with Dirichlet boundary conditions.
The *inverse problem* is, given $\hat{w}$, to find E satisfying

$$-(\hat{w}_x E)_x - (\hat{w}_y E)_y - (\hat{w} E_x)_x - E_{yy} = g \text{ in } \Omega.$$

Considered as second order PDE for E, the principal part is

$$... - \hat{w}E_{xx} - E_{yy}...;$$

hence, the equation for E is

• elliptic where $\hat{w} > 0$

• hyperbolic where $\hat{w} < 0$.

The special case $\hat{w}(x, y) = y$ leads to the Tricomi equation (see e.g. [24]).
In [22], the numerical solution of this inverse problem by Landweber iteration and the numerical results are described in detail. Since the inverse problem is a second order PDE for E, also boundary conditions have to be imposed on E (where the answer to the question which conditions should be imposed depends on the type of this PDE). In the following results, E was fixed on the boundary. For this case, a basic observation was that Landweber iteration converges much faster in the purely elliptic case, where the PDE for E is elliptic everywhere (symbolized by a broken line in Figures 9 and 10) compared to the purely hyperbolic case (the solid lines in Figures 9 and 10), and the final accuracy is of about one order of magnitude better (which is understandable since boundary conditions for E are appropriate in the elliptic but not in the hyperbolic case):

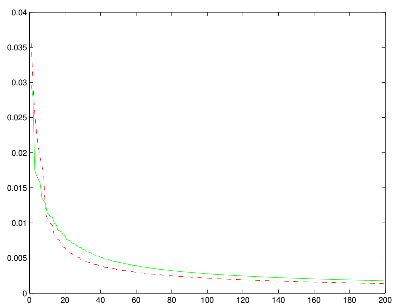

Figure 9: $\frac{\|\hat{w} - w(E_k)\|_{L^2(\Omega)}}{\|\hat{w}\|_{L^2(\Omega)}}$ vs. k

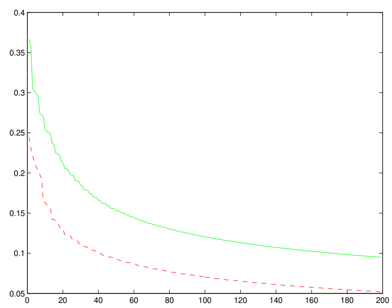

Figure 10: $\frac{\|E - E_k\|_{H^1(\Omega)}}{\|E\|_{H^1(\Omega)}}$ vs. k

Interestingly, the error structure in the final iteration is markedly different between the elliptic and hyperbolic cases:

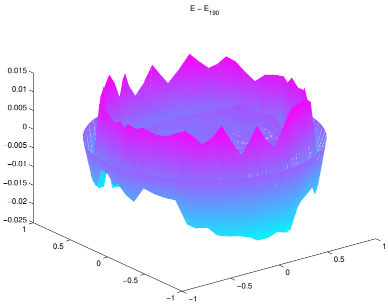

Figure 11: $E - E_{190}$, elliptic case

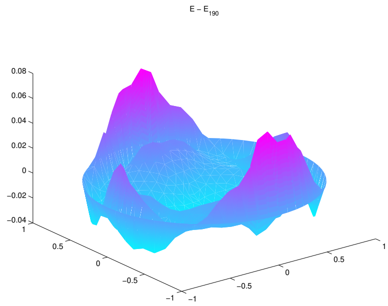

Figure 12: $E - E_{190}$, hyperbolic case

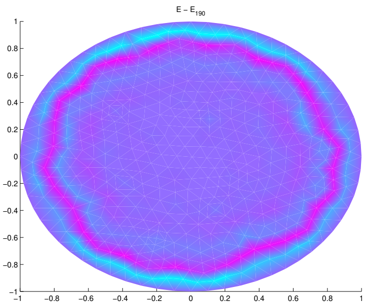

Figure 13: $E - E_{190}$, elliptic case, top view

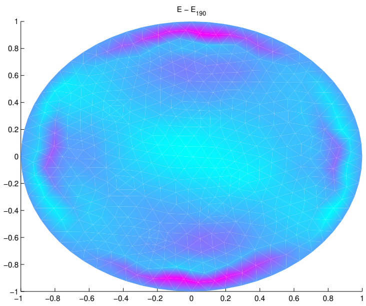

Figure 14: $E - E_{190}$, hyperbolic case, top view

With noisy data, we obtain the typical "semi–convergence" behaviour (cf. Section 5), i.e., the error first decreases and then increases again due to propagated noise:

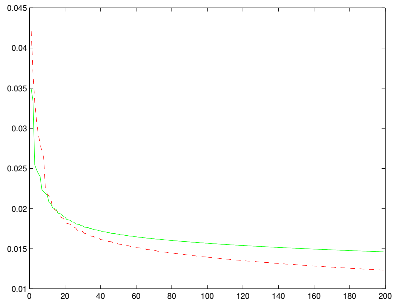

Figure 15: $\frac{\|\hat{w}^\delta - w(E_k)\|_{L^2(\Omega)}}{\|\hat{w}\|_{L^2(\Omega)}}$ vs. k

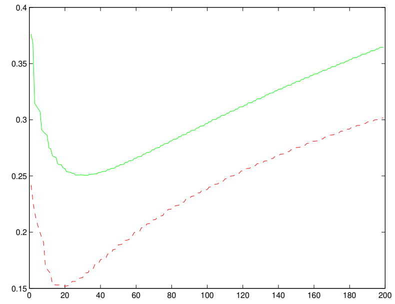

Figure 16: $\frac{\|E - E_k\|_{H^1(\Omega)}}{\|E\|_{H^1(\Omega)}}$ vs. k

A case where the equation for E is hyperbolic for $x < 0$ and elliptic for $x > 0$ ($\hat{w}(x, y) = x$, so that the equation for E is a Tricomi–type equation) is shown in the next figure:

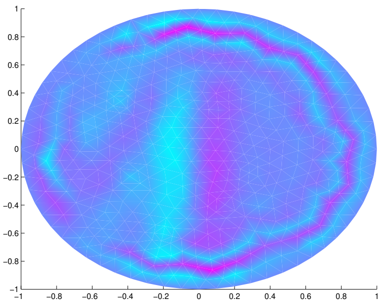

Figure 17: $E - E_{190}$, mixed case, top view

Comparing this picture with the characteristics of the PDE for E, one sees that there must be some connection. However, we are not (yet) able to say precisely what this connection is.

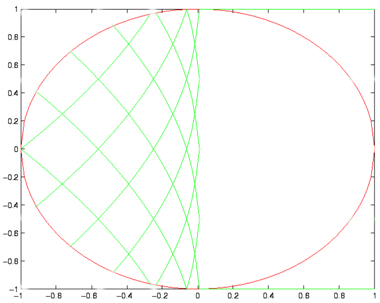

Figure 18: characteristics for $\hat{w} = x$

This problem certainly needs more analysis. A conclusion of these numerical arguments is certainly that for a parameter identification problem which is of second order in the unknown parameter, mathematical properties of the PDE fulfilled by E play a role even if this PDE is not directly used as in the output–least–squares approach. Thus, parameter identification problems where second derivatives of the parameter appear as the identification of Young's modulus in the plate equation from elasticity show some new features compared to more traditional parameter identification problems where the parameter appears with first derivatives at most.
We finally mention a new and quite promising approach to parameter identification which somehow combines the output–least–squares and the equation–error approaches, namely the minimization of the output defect subject to the equation considered as equality constraint by Sequential Quadratic Proramming ([13], [14]).

References

[1] G. Alessandrini, E. Beretta, E. Rosset, S. Vessella, Optimal stability for elliptic boundary value problems with unknown boundaries, Ann. Scuola Norm. Sup. Pisa 29 (2000), 755-806

[2] R.S. Anderssen, H.W. Engl, O. Scherzer, Parameter identification from boundary measurements in a parabolic equation arising from geophysics, Nonlinear Analysis 20 (1993), 127-156

[3] A. B. Bakushinskii, The problem of the convergence of the iteratively regularized Gauss-Newton method, Comput. Math. Math. Phys. 32 (1992), 1353-1359

[4] H. Banks, K. Kunisch, Parameter Estimation Techniques for Distributed Systems, Birkhäuser, Boston, 1989

[5] A. Binder, C.W. Groetsch, A. Neubauer, O. Scherzer, Weakly closed nonlinear operators and parameter identification in parabolic equations by Tikhonov regularization, Applicable Analysis 55(1994), 215-234

[6] R.M. Brown, G.A. Uhlmann, Uniqueness in the inverse conductivity problem for nonsmooth conductivities in two dimensions, Commun. Part. Diff. Equ. 22 (1997), 1009-27

[7] M. Burger, Iterative regularization of a parameter identification problem occurring in polymer crystallization, SIAM J. Numer. Anal. 39 (2001), 1029-1054

[8] M. Burger, V. Capasso, G. Eder, Modelling crystallization of polymers in temperature fields, ZAMM 82 (2001), 51-63

[9] M. Burger, Direct and Inverse Problems in Polymer Crystallization Processes, Dissertation, Johannes Kepler Universität Linz, 2000

[10] M. Burger, A. Micheletti, Stochastic and deterministic simulation of nonisothermal crystallization of polymers J. Math. Chem. (2002), to appear

[11] M. Burger, V. Capasso, H.W. Engl, Inverse problems related to crystallization of polymers, Inverse Problems 15 (1999), 155-173

[12] M. Burger, H.W. Engl, P.A. Markowich, P. Pietra, Identification of doping profiles in semiconductor devices, Inverse Problems 17 (2001), 1765-1795

[13] M. Burger, W. Mühlhuber, Iterative regularization of parameter identification problems by SQP methods, Universität Linz, SFB F013 Report 01-18 (2001), and submitted

[14] M. Burger, W. Mühlhuber, Numerical approximation of an SQP-type method for parameter identification, Universität Linz, SFB F013 Report 01-19 (2001), and submitted

[15] D. Colton, R. Kress, Integral Equation Methods in Scattering Theory, Wiley, New York, 1983

[16] P. Deuflhard, H.W. Engl, and O. Scherzer, A convergence analysis of iterative methods for the solution of nonlinear ill-posed problems under affinely invariant conditions, Inverse Problems 14 (1998), 1081-1106

[17] P. Deuflhard, G. Heindl, Affine invariant convergence theorems for Newton's method and extensions to related methods, SIAM J. Numer Anal. 16 (1979), 1081-1106

[18] K. Kunisch, A. Neubauer, Convergence rates for Tikhonov regularization of nonlinear ill-posed problems, Inverse Problems 5 (1989), 523-540

[19] H.W. Engl, H. Gfrerer, A posteriori parameter choice for general regularization methods for solving linear ill-posed problems, Appl.Num.Math. 4 (1988), 395-417

[20] H.W. Engl, K. Kunisch, O. Scherzer, Optimal a-posteriori parameter choice for Tikhonov regularization for solving nonlinear ill-posed problems, SIAM Journal on Numerical Analysis 30 (1993), 1796- 1838

[21] H.W. Engl, P. Kügler, Identification of a temperature dependent heat conductivity by Tikhonov regularization, J. of Inverse and Ill-Posed Problems (2002), to appear

[22] H.W. Engl, P. Kügler, The influence of the equation type on iterative parameter identification problems which are elliptic or hyperbolic in the parameter, Europ. J. of Appl. Math., to appear

[23] H.W. Engl, O. Scherzer, Convergence rates results for iterative methods for solving nonlinear ill-posed problems, in: D. Colton, H.W. Engl, A.K. Louis, J. McLaughlin, W.F. Rundell (eds.), Survey on Solution Methods for Inverse Problems, Springer, Vienna/New York, 2000, 7-34

[24] J. Ockendon, S. Howison, A. Lacey, M. Movchen, Applied Partial Differential Equations, Oxford University Press, Oxford, 1999

[25] H.W. Engl, J. Zou, Stability and convergence analysis of Tikhonov regularization for parameter identification in a parabolic equation, Inverse Problems 16 (2000), 1907-1923

[26] C.W. Groetsch, The Theory of Tikhonov Regularization for Fredholm Equations of the First Kind, Pitman, Boston, 1984

[27] M. Hanke, A regularizing Levenberg-Marquardt scheme, with applications to inverse groundwater filtration problems, Inverse Problems 13 (1997), 79-95

[28] M. Hanke, A. Neubauer, O. Scherzer, A convergence analysis of the Landweber iteration for nonlinear ill-posed problems, Numer. Math. 72 (1995), 21-37

[29] B. Hofman, O. Scherzer, Local ill-posedness and source conditions of operator equations in Hilbert spaces, Inverse Problems 14 (1998), 1189-1206

[30] T. Hohage, Convergence rates of a regularized Newton method in sound-hard inverse scattering. SIAM J. Numer. Anal. 36 (1998), 125-142

[31] T. Hohage, Iterative Methods in Inverse Obstacle Scattering: Regularization Theory of Linear and Nonlinear Exponentially Ill-Posed Problems, PhD Thesis, Universität Linz, 1999

[32] H.W. Engl, M. Hanke, A. Neubauer, Regularization of Inverse Problems, Kluwer, Dordrecht 1996

[33] B. Kaltenbacher, A posteriori parameter choice strategies for some Newton type methods for the regularization of nonlinear ill-posed problems, Numer. Math. 79 (1998), 501-528

[34] B. Kaltenbacher, Some Newton type methods for the regularization of nonlinear ill-posed problems, Inverse Problems 13 (1997), 729-753

[35] M. Lavrentiev, Some Improperly Posed Problems of Mathematical Physics, Springer, New York, 1967

[36] S. Manservi, M. Gunzburger, A variational inequality formulation on an inverse elasticity problem, Appl. Num. Math. 34 (2000), 99-126

[37] P. Markowich, The Stationary Semiconductor Device Equations, Springer, Vienna, 1986

[38] A.I. Nachman, Global uniqueness for a two-dimensional inverse boundary value problem, Ann. Math. 143 (1996), 71-96

[39] R. Ramlau, A modified Landweber-method for inverse problems, Num. Funct. Anal. Opt. 20 (1999), 79-98

[40] E. Schock, T. Nair, On the Ritz method and its generalizations for ill-posed equations with non-selfadjoint operators, in preparation

[41] E. Schock, Approximate solution of ill-posed equations: arbitrarily slow convergence vs. superconvergence, in: G. Hämmerlin and K. H. Hoffmann, eds., Constructive Methods for the Practical Treatment of Integral Equations, Birkhäuser, Basel, 1985, 234-243

[42] T.I. Seidman, C.R. Vogel, Well-posedness and convergence of some regularization methods for nonlinear ill-posed problems, Inverse Problems 5 (1989), 227-238

[43] A.N. Tikhonov and V. Arsenin, Solutions of Ill-Posed Problems, Wiley, New York, 1977